BNL-226378-2024-TECH

EIC-ADD-TN-113

Space Charge Effects on Spin Polarization in High-Intensity Preinjector

E. Wang

November 2024

Electron-Ion Collider

Brookhaven National Laboratory

U.S. Department of Energy

USDOE Office of Science (SC), Nuclear Physics (NP)

DISCLAIMER

Space Charge Effects on Spin Polarization in High-Intensity Preinjector

Erdong Wang* and Jyoti Biswas
Brookhaven National Laboratory, Upton, NY 11973,USA
(Dated: Original version: Nov. 12, 2024, updated version: Jan. 2, 2025)

This analytical study investigates the space charge impact on electron beam polarization within the low-energy range, spanning from the polarized electron gun up to the linac. The research study three sections: the gun-to-Wien filter interface, the Wien filter section, and the bunching section. We will comprehensively assess polarization degradation mechanisms in each region characterized by space charge effects. Then we performed the spin tracking through the entire low-energy transmission system using a General Particle Tracer (GPT) to validate our analytical findings and include the higher-order components.

I. INTRODUCTION

In the Electron-Ion Collider (EIC), we propose utilizing a Wien filter as a spin rotator to transform electron spin orientation from longitudinal to vertical at an energy range of 300-320 keV [1, 2]. While Wien filters have been extensively employed in hadron and electron machines for velocity selection and spin rotation, this application represents a novel approach for high-intensity bunches within a high-space charge-dominated region. Table.I shows the Wien filters used in the various facilities and the last line shows the EIC Wien filter parameters. All existing Wien filters are operated at pico or sub-Pico Coulomb bunch charge which space charge can be ignored. We performed the spin dynamics simulation using Zgoubi code, which doesn't include the space charge[3]. These studies have not addressed the unique challenges of such intense beams that would be used at the EIC.

The particles' spin evolution can be described by the Thomas-BMT equation[9].

$$\frac{d\vec{P}}{dt} = \vec{\Omega_0} \times \vec{P} \tag{1}$$

$$\vec{\Omega_0} = -\frac{Ze}{m\gamma}[(1+G\gamma)\vec{B_\perp} + (1+G)\vec{B_\parallel} + (G\gamma + \frac{\gamma}{1+\gamma})\frac{\vec{E}\times\vec{v}}{c^2}] \tag{2}$$

Where $\vec{P}$ is defined in the particle rest frame and $\vec{E}$ and $\vec{B}$ are defined in the laboratory frame. And $\vec{B}$ gives $\vec{B} = \vec{B}_\perp + \vec{B}_\parallel, \vec{B}_\parallel = (\vec{v}\cdot\vec{B})\vec{v}/v^2$ where $\vec{B}_\parallel$ parallel to the beam velocity, $G = \frac{g-2}{2}$ is the anomalous magnetic moment. For electrons, $G = 0.001159$.

The transverse space charge forces E_r and B_φ contribute to the variation of the spin vector $\vec{P}$ according to the Thomas-BMT equation Eq. 2. While the longitudinal space charge force $\vec{E_z} \times \vec{v} = 0$, it generates an energy spread that impacts spin polarization. This note is structured in the following way:

1. Calculate the transverse space charge E_r and B_φ in uniform distribution and Gaussian distribution.

2. Show the spin process in the Wien filter and calculate the EIC Wien filter parameters.

Name	Energy (keV)	Bunch charge (pC)	Plate length (cm)	Gap (cm)	E_y (MV/m)	B_x (mT)	Feedthrough (kV)
CEBAF[4]	130	2	32.28	1.5	1.6	9.1	12.4
CEBAF[5]	200	2.7	32.28	1.5	2.7	13	17.5
S-DALINAC[6]	100	4	38.10	2.0	0.756	4.6	12
MAMI[7]	100	0.02	32	2.0	1.07	6.56	12.5
EIC[8]	320	7-14 $\times 10^3$	45.92	7.0	1.44	6.080	50.5

TABLE I: An overview of the Wien filters in operation for the electron spin rotation

* wange@bnl.gov

3. Calculated the longitudinal space charge force E_Z induced energy spread and evaluates energy spread-induced polarization degradation inside the Wien filter

4. Calculated transverse space charge force-induced polarization degradation in the Wien filter

5. Calculated transverse space charge force-induced polarization degradation in the preinjector into three sections: before the Wien filter, ballistic compression, and across chicane compression.

II. SPACE CHARGE FORCES

We discuss the space charge forces for the two parts: I) Transverse space charge; and II) Longitudinal space charge. The transverse space charge force can be driven by Gauss's law and Ampere's law which gives

$$\int_S \vec{E} \cdot \hat{n} dS = \frac{q}{\varepsilon_0} \tag{3}$$

$$\oint_l \vec{B} \cdot \vec{l} = \mu_0 I \tag{4}$$

The beam from the gun initially uses a one-sigma cut-off truncated Gaussian distribution, approximating a uniform distribution. As the beam propagates to the Wien filter, transverse space charge effects cause the beam's transverse distribution to evolve towards a Gaussian distribution. Consequently, our analysis will examine the electric and magnetic force under both uniform and Gaussian distribution scenarios.

A. Uniform distribution

For the uniform distribution, the charge density is

$$\lambda(r) = \lambda_0 (\frac{r}{a})^2 \tag{5}$$

where $\lambda_0 = \frac{Q}{\beta ct} = \frac{I}{\beta c}$ is the charge density with unit of C/m. I is the current with the unit of A. Here using the coasting beam, the Q is the charge, other than the bunch charge.

First, we get the transverse electric field by

$$2\pi r \Delta z E_r = \frac{\lambda(r)\Delta z}{\varepsilon_0} \tag{6}$$

$$E_r = \frac{\lambda_0 r}{2\pi\varepsilon_0 a^2} = \frac{I Z_0}{2\pi\beta}\frac{r}{a^2} \tag{7}$$

where $Z_0 = \sqrt{\frac{\mu_0}{\varepsilon_0}} = \frac{1}{c\varepsilon_0} = 377(\Omega)$

Then, we get the transverse magnetic field by

$$2\pi r B_\varphi = \mu_0 J \pi r^2 = \mu_0 \beta c \lambda(r) \tag{8}$$

$$B_\varphi = \frac{\mu_0 \beta c^2 \lambda_0}{2\pi r c}\frac{r^2}{a^2} \tag{9}$$

$$= \frac{\lambda_0 \beta}{2\pi\varepsilon_0 c}\frac{r}{a^2} \tag{10}$$

$$= \frac{Z_0 I}{2\pi c}\frac{r}{a^2} \tag{11}$$

Equations 7 and 11 show the electric and magnetic transverse space charge forces with the uniform distribution.

B. Gaussian distribution

Let's get the transverse space charge in Gaussian distribution. The density of a Gaussian bunch is given by

$$\rho(r,z) = \frac{Q}{\sqrt{2\pi}^3 \sigma_z \sigma_r^2} e^{-\frac{z^2}{2\sigma_z^2}} e^{-\frac{r^2}{2\sigma_r^2}} \tag{12}$$

where Q is the bunch charge, σ_z, σ_r are the longitudinal and transverse Gaussian standard deviations, respectively. Using Eq. 12,$\frac{Q}{\sqrt{2\pi}\sigma_z} = \frac{I_{pk}}{\beta c}$ and Gauss's Law, we have the transverse space charge electric field

$$E_r = \frac{1}{2\pi\varepsilon_0} \frac{Q}{\sqrt{2\pi}\sigma_z\sigma_r^2} e^{-\frac{z^2}{2\sigma_z^2}} \int_0^r e^{\frac{r'^2}{2\sigma_r'^2}} r' dr' \tag{13}$$

$$= \frac{1}{2\pi\varepsilon_0} \frac{Q}{\sqrt{2\pi}\sigma_z\sigma_r^2} e^{-\frac{z^2}{2\sigma_z^2}} \frac{1 - e^{-\frac{r^2}{2\sigma_r^2}}}{r} \tag{14}$$

$$= \frac{1}{2\pi\beta c\varepsilon_0} I_{pk} e^{-\frac{z^2}{2\sigma_z^2}} \frac{1 - e^{-\frac{r^2}{2\sigma_r^2}}}{r} \tag{15}$$

$$= \frac{I_{pk} Z_0}{2\pi\beta r} e^{-\frac{z^2}{2\sigma_z^2}} (1 - e^{-\frac{r^2}{2\sigma_r^2}}) \tag{16}$$

Similar as Eq. 11, we can write the B_φ in Gaussian distribution is

$$B_\varphi = \frac{\vec{\beta} \times \vec{E_r}}{c} \tag{17}$$

$$= \frac{I_{pk} Z_0}{2\pi c r} e^{-\frac{z^2}{2\sigma_z^2}} (1 - e^{-\frac{r^2}{2\sigma_r^2}}) \tag{18}$$

C. Initial beam parameters

The Wien filters are positioned after the gun dipole, approximately 2-3 meters from the photocathode. At this location, the approximate beam parameters are detailed in Table II. The space charge transverse electric field E_r and magnetic field B_φ of the uniform distribution and Gaussian distribution are illustrated in Fig. 1a and 1b, respectively.

	Parameters
Bunch Charge	7.5 nC
Bunch length	1.3 ns (HMFW, beercan with 150 ps rising time)σ_z=0.7 ns
Beam size radius	10 mm (Guassian σ_r) or 20 mm (Uniform r_{max})
Beam energy	320 keV
Peak Current for Gaussian	4.27 A

TABLE II: Beam parameter in the Wien filter range

III. SPIN ROTATION IN THE WIEN FILTER

A Wien filter model is shown in Fig. 2.

The Wien filter serves two primary functions: electron velocity filtering and spin direction rotation. The EIC Wien filter only functions as a spin rotator and makes the electron beam go through as much as possible. The electric and magnetic fields are perpendicular, allowing the Lorentz force to be balanced by the static electric force. Consequently,

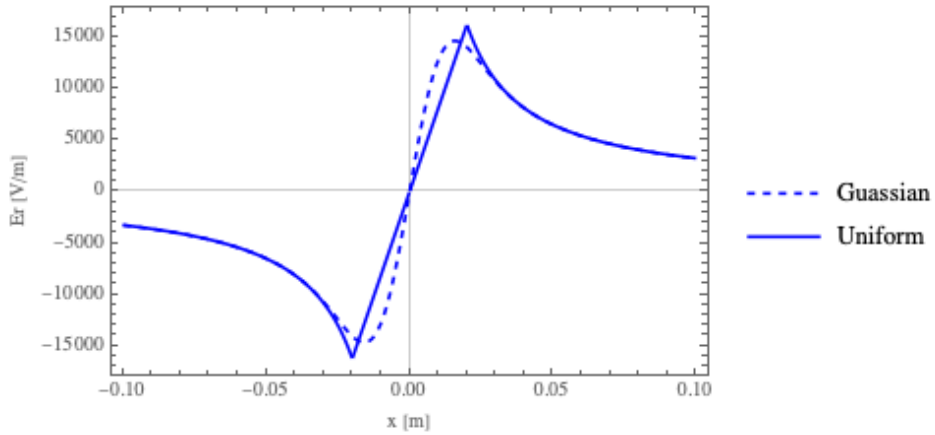

(a) The transverse space charge electrical field in Gaussian and uniform distribution

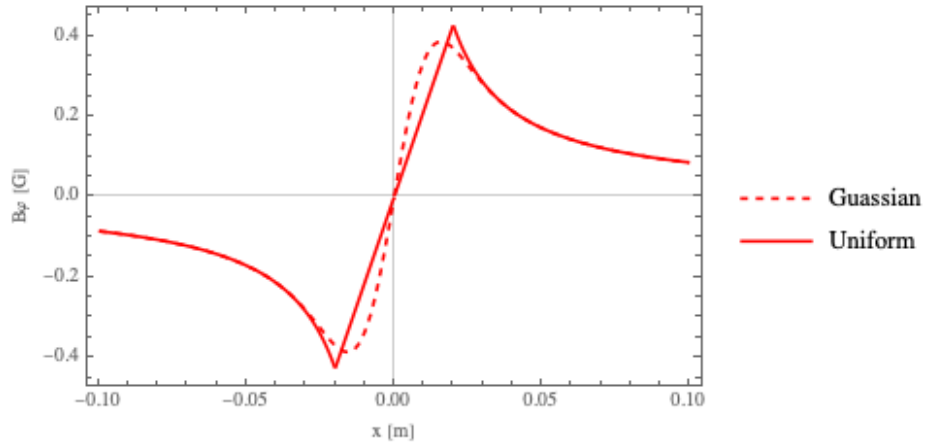

(b) The transverse space charge magnetic field in Gaussian and uniform distribution

FIG. 1: The transverse space charge electric and magnetic field in Gaussian and uniform distribution

we can derive the following equations

$$\vec{E} + \vec{v} \times \vec{B} = 0 \tag{19}$$

$$E_y = -v_z B_x \tag{20}$$

$$qv_z B_x = \frac{\gamma m_0 v_z^2}{\rho} \tag{21}$$

$$\frac{\vec{E} \times \vec{v}}{c^2} = \frac{1-\gamma^2}{\gamma^2} \vec{B}_\perp \tag{22}$$

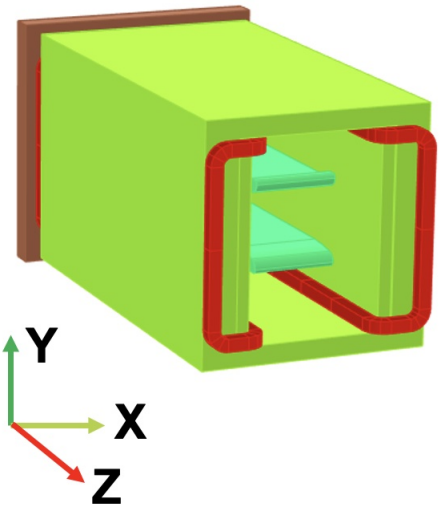

FIG. 2: Perspective view of the Opera 3D model of the Wien filter. Nickel plates are used on both sides to shape the fringe B-field. The front-side Nickel plate is not shown here to make the electrodes visible.

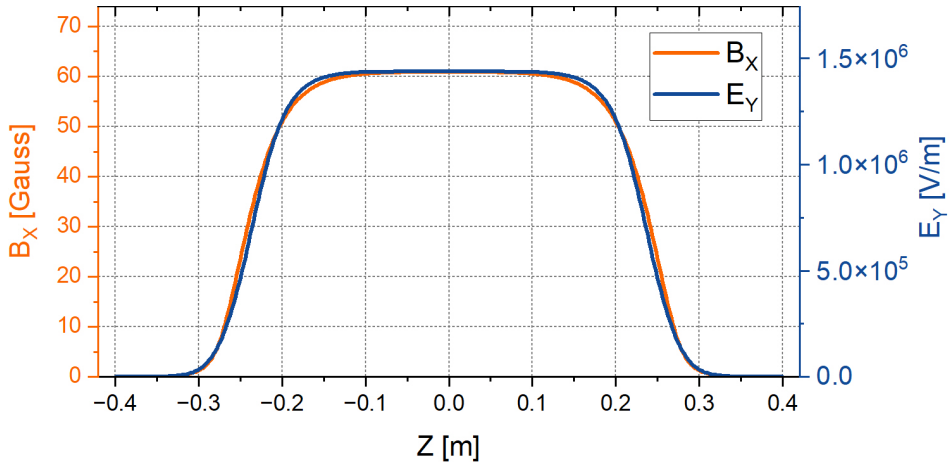

FIG. 3: Simulated electric and magnetic field generated from Opera 3D at the center-line.

Insert these equation into the Eq. 2, and $\vec{B}_{\parallel} = 0$, then we have

$$\overrightarrow{\Omega}_0 = -\frac{q}{m\gamma}\{(G\gamma + \frac{\gamma}{\gamma+1})\frac{1-\gamma^2}{\gamma^2}]\vec{B}_{\perp} + (1+G\gamma)\vec{B}_{\perp}\} \tag{23}$$

$$= -\frac{q}{m\gamma}\frac{1}{\gamma}(G - G\gamma^2 + 1 - \gamma + \gamma + G\gamma^2)\vec{B}_{\perp} \tag{24}$$

$$= \frac{q}{m\gamma^2}(G+1)\vec{B}_{\perp} \tag{25}$$

$$\overrightarrow{P} = \int_T \frac{q}{m\gamma^2}(G+1)\vec{B}_{\perp}dt \tag{26}$$

$$= \frac{q(G+1)}{mv\gamma^2}\int \vec{B}_{\perp}ds \tag{27}$$

Simplified by Eq. 27, we can get the main Wien filter design parameters by the following equations

$$G = 0.0011 \approx 0 \tag{28}$$

$$W = \frac{dP}{ds} = \frac{qB}{mv\gamma^2}(\text{rad/m}) \tag{29}$$

$$L = \frac{\theta(\text{rad})}{W}(\text{m}) \tag{30}$$

Where W is the spin rotation rate; γ is the relativistic factor; e and m are the electron's charge and mass in SI units; θ is the rotation angle and L is the Wien filter length. Based on this estimation, the EIC preinjector Wien filter conceptual design employs two Wien filters to rotate the spin direction by $\pi/2$. With the feedthrough voltage limited to 50 kV, using Eq. 30, we can determine the EIC Wien filter parameters listed in Table III.

	Parameters
Gap	7 (cm)
B field	6.08 (mT)
E field	1.44 (MV/m)
Length	45.92 (cm)
Energy	320 (keV)
Voltage	50.5 (kV)
Spin rotate angle	$\pi/4$ (rad)

TABLE III: The proposed EIC Wien filter parameters.

IV. POLARIZATION DEGRADATION IN THE WIEN FILTER BY THE ENERGY SPREAD

A. Longitudinal space charge

The beam energy from the gun is 320 keV. The bunch experiences longitudinal space charge effects, which increase the energy spread before entering the Wien filter. The spin rotation rate depends on the beam energy, as shown in Eq. 30. An analytical approach is used to evaluate the energy spread induced by longitudinal space charge and its impact on polarization degradation.

The electrostatic potential and longitudinal electric field are

$$\Phi(r,z) = \int_r^b E_r dr \tag{31}$$

$$E_z = -\frac{\partial \Phi}{\partial z} \tag{32}$$

$$E_z = -\frac{1}{\gamma^2}\frac{\partial}{\partial z}\int_r^b E_r(r,z)dr \tag{33}$$

E_r can be determined using Eqs. 16 and 7. For a Gaussian distribution in the rest frame, solving the integral term $\int_r^b \frac{1}{\gamma r}(1 - e^{-\frac{r^2}{2\sigma_r^2}})$ analytically is challenging without assuming $\gamma = \frac{b}{\sigma_z} \gg 1$, typically $\gamma > 3$[10, 11]. However, in the region between the gun and the Wien filter, $\gamma = 1.6$, $\sigma_z = 1.3$ ns $= 0.39$ m, and $\frac{b}{\sigma_z} = 0.05/0.39 = 0.13$. This clearly shows that our case is far from meeting the $\gamma \gg 1$ assumption.

Given that the laser transverse distribution is a truncated Gaussian with a 1σ cutoff, the beam does not develop into a Gaussian distribution within this section, from the gun to the Wien filter. Therefore, it is appropriate to use a transverse uniform distribution while maintaining a longitudinal Gaussian distribution for calculations in this region. The combination of a longitudinal Gaussian distribution and a transverse uniform distribution can be expressed as follows:

$$E_r = \frac{IZ_0}{2\pi\beta}\frac{r}{a^2}e^{-\frac{z^2}{2\sigma_z^2}} \ (r \le a) \tag{34}$$

$$E_r = \frac{IZ_0}{2\pi\beta}\frac{1}{r}e^{-\frac{z^2}{2\sigma_z^2}} \ (r > a) \tag{35}$$

Consequently, we can find E_z by using Eq. 33

$$E_z = \frac{IZ_0}{2\pi\beta}\left(\int_r^a \frac{r'}{a^2}dr' + \int_a^b \frac{1}{r'}dr'\right)\frac{\partial e^{-\frac{z^2}{2\sigma_z^2}}}{\partial z} \tag{36}$$

$$= \frac{IZ_0}{4\pi\beta}\left(1 - \frac{r^2}{a^2} + 2ln\frac{b}{a}\right)\frac{\partial e^{-\frac{z^2}{2\sigma_z^2}}}{\partial z} \tag{37}$$

$$\tag{38}$$

where b is the beam pipe radius and a is the beam radius[12]. When $r = 0$, we have

$$E_z = -\frac{IZ_0}{4\pi\beta}\left(1 + 2ln\frac{b}{a}\right)\frac{z}{\sigma_z^2}e^{-\frac{z^2}{2\sigma_z^2}} \tag{39}$$

$$F_z = -\frac{eIZ_0}{4\pi\beta}\left(1 + 2ln\frac{b}{a}\right)\frac{z}{\sigma_z^2}e^{-\frac{z^2}{2\sigma_z^2}} \tag{40}$$

$$E(z) = F_z(z)L + E_0 \tag{41}$$

where L is the drift length. E(z) is the electron's energy as the function of the position in the bunch and E_0 is the center electron's energy. Fig. 4a shows the longitudinal space charge electric gradient along the bunch and Gaussian distributions.

B. ESP evaluation

The Electron Spin Polarization (ESP) can be calculated by

$$ESP = \frac{\sum_i^N \left|\vec{P_i}\cdot\vec{P_0}\right|}{N} \tag{42}$$

where P_0 is the desired spin direction, P_i is each electron's spin direction, and N is the number of particles in one bunch.

Using the Eq. 30,we can get ESP

$$ESP = \int_{-\infty}^{\infty}\cos(W(E(z))L)\rho(z)dz \tag{43}$$

Using the parameters in Table II, the ESP impact from the energy spread caused by longitudinal space charge is 0.99959 with the rms energy spread of about 1.8% which matches with Parmela simulation results. We can also obtain the ESP as a function of RMS energy spread, as illustrated in Fig. 5. The energy spread variations are attributed to different peak current values.

V. ESP IMPACTED BY THE TRANSVERSE SPACE CHARGE FORCE IN THE WIEN FILTER

In this section, we will calculate E_r and B_φ impact on the spin independently in the Wien filter.

A. High energy case

For the high energy case where the $\beta = c$ and,$\gamma \gg 1$, the space charge force

$$\vec{F_{sc}} = e(\vec{E_r} - c\vec{\beta}\times\vec{B_\varphi}) \tag{44}$$

$$= \frac{e}{\gamma^2}\vec{E_r} \tag{45}$$

$$\approx 0 \tag{46}$$

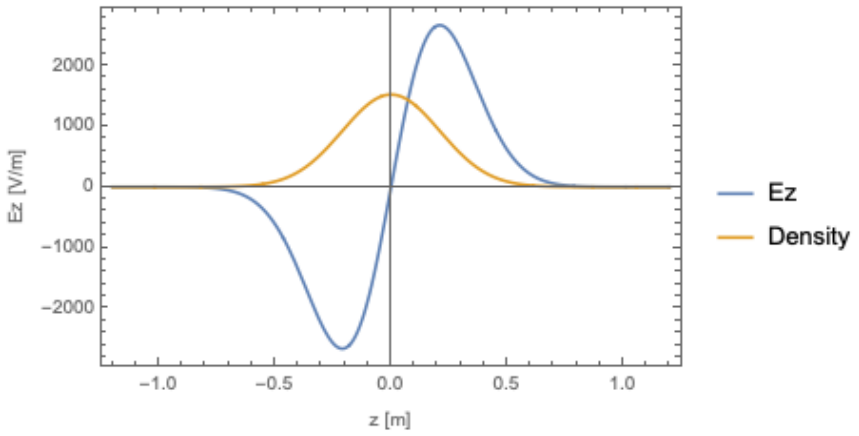

(a) Longitudinal space charge gradient as a function of electron longitudinal position $Ez(z)$ and Gaussian distribution

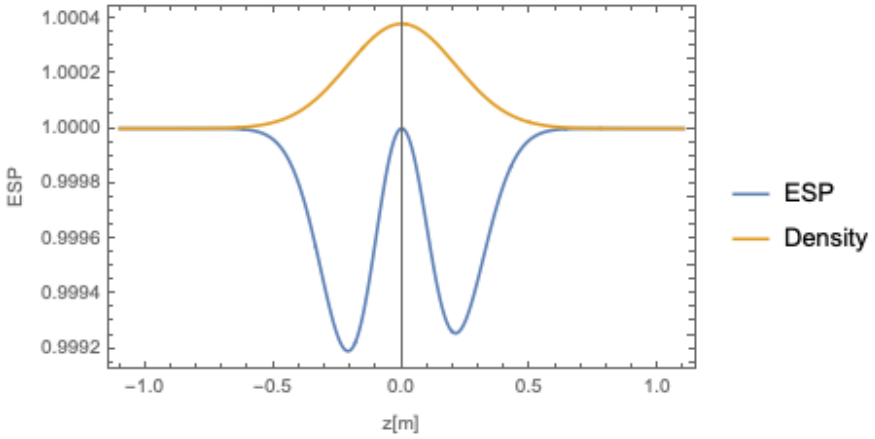

(b) Longitudinal space charge caused ESP degradation as the function of electron longitudinal position and Gaussian distribution

FIG. 4: The longitudinal space charge induces an electric field and impacts the ESP.

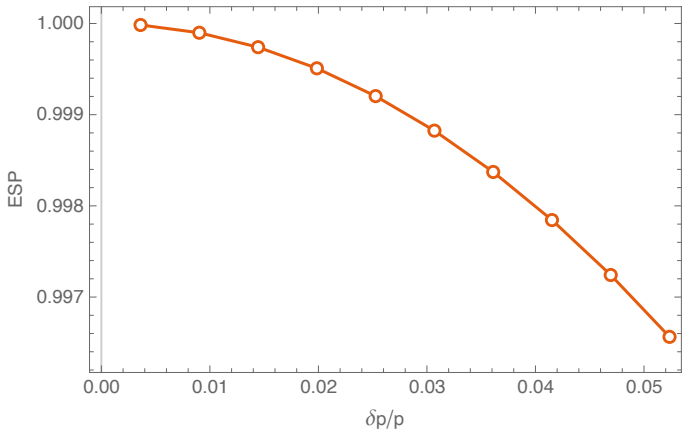

FIG. 5: The ESP as the function of the RMS energy spread.

Then, we have

$$\vec{v} \times \vec{B} + \vec{E} = 0 \tag{47}$$
$$\vec{v} \times (\vec{v} \times \vec{B}) = \vec{E} \times \vec{v} \tag{48}$$
$$(\vec{v} \cdot \vec{B})\vec{v} - \vec{v}^2\vec{B} = \vec{E} \times \vec{v} \tag{49}$$
$$-v^2\vec{B} = \vec{E} \times \vec{v} \tag{50}$$

Put Eq. 50 into Eq. 2, when $\beta \approx 1$,we have

$$\vec{\Omega_0} = -\frac{q}{m\gamma}(1+G\gamma)(\vec{B_\varphi} + \frac{\vec{E} \times \vec{v}}{c^2}) = -\frac{q}{m\gamma}(1+G\gamma)\vec{B_\varphi}(1 - \frac{v^2}{c^2}) \approx 0 \tag{51}$$

B. Low energy case

For the low-energy case, the space charge is strong. We use Eq. 2 and Eq. 18, which can write the spin direction change either by the function of B_φ

$$\frac{d\vec{P}}{dt} = -\frac{e}{m\gamma}\left[(1+G\gamma)\vec{B}_\varphi + \left(G\gamma + \frac{\gamma}{1+\gamma}\right)\frac{\vec{E}_r \times \vec{v}}{c^2}\right] \times \vec{P} \tag{52}$$
$$= -\frac{e}{m\gamma}\left[(1+G\gamma)\vec{B}_\varphi \times \vec{P} + \left(G\gamma + \frac{\gamma}{1+\gamma}\right)\frac{\vec{E}_r \times \vec{v}}{c^2} \times \vec{P}\right] \tag{53}$$
$$= -\frac{e}{m\gamma}\left[(1+G\gamma)\vec{B}_\varphi \times \vec{P} - \left(G\gamma + \frac{\gamma}{1+\gamma}\right)\vec{B}_\varphi \times \vec{P}\right] \tag{54}$$
$$= -\frac{e}{m\gamma}\left[\left(1 - \frac{\gamma}{1+\gamma}\right)\vec{B}_\varphi \times \vec{P}\right] \tag{55}$$
$$\frac{d\vec{P}}{ds} = -\frac{e}{\beta cm\gamma}\left[\left(1 - \frac{\gamma}{1+\gamma}\right)\vec{B}_\varphi \times \vec{P}\right] \tag{56}$$
$$\tag{57}$$

or by the function of E_r

$$\frac{d\vec{P}}{ds} = \frac{e}{\beta cm\gamma}\left[\left(1 - \frac{\gamma}{1+\gamma}\right)\frac{\vec{E}_r \times \vec{v}}{c^2} \times \vec{P}\right] \tag{58}$$

B_φ is the function of the particle's position r and z as shown in Eq. 18. Let's estimate a simple case as an electron particle at one σ of a Gaussian distribution. The magnetic field, B_φ, is 0.33 Gauss and the Lorentz factor, γ, is 1.62. The polarization vector, $\vec{P}$, is longitudinal from the source, and thus from Eq. 57, $\frac{d\vec{P}}{ds} = 0.21°$. This represents the upper limit, as the spin direction evolves into the vertical within the Wien filter as well as $\vec{B}_\varphi$ depends on φ, the cross product $\vec{B}_\varphi \times \vec{P}$ can become smaller.

Now, let's evaluate the deterioration of the ESP through the Wien filter, taking into account the dependencies on φ and $\vec{P}$.

Because the spin vector $\vec{P}$ is changing in the Wien filter, we can write the spin direction as the function of the travel length in the Wien filter. From Eq. 30, we have $\vec{P} = \frac{l}{L}\pi/2$, where l is the electron travel length and L is the

Wien filter total length. We let spin angle $\theta = \frac{l}{L}\frac{\pi}{2}$ and have

$$\vec{P} = \cos(\theta)\,\hat{z} - \sin(\theta)\,\hat{y} \tag{59}$$

$$\vec{B}_\varphi = B_\varphi\left[\cos(\varphi)\,\hat{x} - \sin(\varphi)\,\hat{y}\right] \tag{60}$$

$$\vec{B}_\varphi \times \vec{P} = B_\varphi \begin{vmatrix} \hat{x} & \hat{y} & \hat{z} \\ \cos\varphi & -\sin\varphi & 0 \\ 0 & -\sin\theta & \cos\theta \end{vmatrix} \tag{61}$$

$$= \left[-\cos(\theta)\sin(\varphi)\,\hat{x} - \cos(\varphi)\cos(\theta)\,\hat{y} - \cos(\varphi)\sin(\theta)\,\hat{z}\right] B_\varphi \tag{62}$$

Then we can integral the dP through the entire Wien filter using Eq. 57 as

$$\Delta\vec{P} = \int_0^L \frac{e}{\beta cm\gamma}\left[\left(1 - \frac{\gamma}{1+\gamma}\right)\vec{B}_\varphi \times \vec{P}\right] ds \tag{63}$$

$$= \frac{e}{\beta cm\gamma}\left(1 - \frac{\gamma}{1+\gamma}\right) B_\varphi \int_0^L \cos\left(\frac{s}{L}\frac{\pi}{2}\right)\sin(\varphi)\,\hat{x} + \cos\left(\frac{s}{L}\frac{\pi}{2}\right)\cos(\varphi)\,\hat{y} + \sin\left(\frac{s}{L}\frac{\pi}{2}\right)\cos(\varphi)\,\hat{z}\,ds \tag{64}$$

$$= \frac{e}{\beta cm\gamma}\left(1 - \frac{\gamma}{1+\gamma}\right) B_\varphi \frac{2L}{\pi}\left(\sin\varphi\,\hat{x} + \cos\varphi\,\hat{y} + \cos\varphi\,\hat{z}\right) \tag{65}$$

$$\tag{66}$$

Let $\frac{e}{\beta cm\gamma}\left(1 - \frac{\gamma}{1+\gamma}\right)\frac{2L}{\pi} = k$ with unit of $\frac{C\cdot s}{kg}$, .From the Table II. We have $k = 110.9(\frac{C\cdot s}{kg})$ and B_φ is in scale of 10^{-5}(T), So $kB_\varphi \ll 1$.At the exit of the Wien filter the $\vec{P_0} = \hat{y}$. We can calculate ESP using Eq. 42

$$\mathrm{ESP} = \int \frac{(\vec{P_0} + \Delta\vec{P}(r,z))\cdot\vec{P_0}}{\left|\vec{P_0} + \Delta\vec{P}(r,z)\right|\left|\vec{P_0}\right|}\,\rho(r,z) r\,d\varphi\,dr\,dz \tag{67}$$

$$= \int_0^{2\pi}\int_0^\infty\int_{-\infty}^\infty \frac{\left[\hat{y} + kB_\varphi\left(\sin\varphi\,\hat{x} + \cos\varphi\,\hat{y} + \cos\varphi\,\hat{z}\right)\right]\cdot\hat{y}}{\left|\hat{y} + kB_\varphi\left(\sin\varphi\,\hat{x} + \cos\varphi\,\hat{y} + \cos\varphi\,\hat{z}\right)\right|}\,\rho(r,z)\,r\,d\varphi\,dr\,dz \tag{68}$$

$$= \int_0^{2\pi}\int_0^\infty\int_{-\infty}^\infty \frac{1 + kB_\varphi\cos\varphi}{\sqrt{(kB_\varphi)^2 + \left(1 + kB_\varphi\cos\varphi\right)^2}}\,\rho(r,z)\,r\,d\varphi\,dr\,dz \tag{69}$$

$$\approx 2\pi\int_0^\infty\int_{-\infty}^\infty \left(1 - \frac{\left(kB_\varphi\right)^2}{2}\right)\rho(r,z)\,r\,dr\,dz \tag{70}$$

It is reasonable to assume Gaussian distribution, using the Eq. 12, 70 and, we have $ESP = 0.9999962$.

VI. SPIN IMPACTED BY THE TRANSVERSE SPACE CHARGE FORCE IN THE BUNCHING SECTION UP TO THE LINAC

In the front end of the preinjector, after the Wien filter, the spin direction is always vertical, $\vec{P} = \hat{y}$, except for minor wiggling within the solenoids. The solenoid length is approximately 5% of the total length of the front end, so we neglect the solenoids. We divide the front end into the following three sections as listed in Table IV.

Equation 62 can be simplified due to $\vec{P} = \hat{y}$.

$$\vec{B}_\varphi \times \vec{P} = \cos(\varphi)\,\hat{z}B_\varphi \tag{71}$$

The spin direction change due to space charge, similar to Eq. 66 can be rewritten by

$$\Delta\vec{P} = \frac{e}{\beta cm\gamma}\left(1 - \frac{\gamma}{1+\gamma}\right) B_\varphi L\cos\varphi\,\hat{z} \tag{72}$$

Section	Energy	Bunch length	drift length	Polarization
Section 1 (Gun to ballistic bunching)	320 (keV)	1.3 (ns)	6.5 (m)	0.99961
Section 2 (Ballistic bunching to chicane)	3 (MeV)	10 (ps)	2 (m)	0.998872
Section 3 (After chicane compression)	55 (MeV)	2.9 (ps)	7 (m)	0.999997

TABLE IV: The front end preinjector beam parameters split into the three major sections.

Following the procedure of getting Eq. 70, we have the ESP as

$$ESP \approx 2\pi \int_0^\infty \int_{-\infty}^\infty \left(1 - \frac{\left(kB_\varphi\right)^2}{2}\right) \rho(r,z)\, r\, dr\, dz \tag{73}$$

where $k = \frac{e}{\beta cm\gamma}\left(1 - \frac{\gamma}{1+\gamma}\right) L$. The calculated ESP for each section is listed in Table IV.

VII. SPIN TRACKING

The analysis discussed above primarily focuses on the space charge effect, without accounting for beam emittance or other factors such as Wien filter field non-uniformity and solenoid/quadrupole focusing element. A more comprehensive simulation study, utilizing GPT (v3.5) [13], incorporating space charge and spin tracking was preformed.

The gun field, solenoids, quadrupole, and Wien filters field are generated from external codes: Possion, and Opera 3D. To shape the electric field in the fringe region, a Rogowski profile is employed at the end of the electrode plate. The electric and magnetic fields have different decay characteristics, so nickel plates are used to suppress the B-field in the fringe region, ensuring proper matching with the E-field in that region. Opera 3D electrostatic and magnetostatic solvers are used separately to simulate the electric and magnetic fields of the Wien filter, and results are exported in grid format for use in General Particle Tracer (GPT) and Parmela. Details of the Parmela beam dynamics simulations are discussed elsewhere[14]. Fig. 3 shows well-matched Ey and Bx components along the center line. The electrode plate width and the transverse shaping of the iron core are optimized to achieve field matching not only along the center line but also in the transverse direction. In GPT simulation, a realistic field map of 320 kV of the EIC polarized gun is utilized. Two Wien filters were placed after the solenoid and 16° bending. Quadrupole lenses in triplet configuration are used before and in between the Wien filters. A thin quadrupole lens was devised in Opera 3D, and field data including the fringe fields were imported into GPT for beam dynamics and spin tracking simulation.

The GPT output includes each particle's 6D phase space and spin direction on both timesteps and position detectors which are set up in the GPT input field. In our case, the spin direction (S_x, S_y, S_z) was measured at 1 cm intervals in GPT 3.5. A spin length of unity in GPT represents a fully polarized particle, whereas a spin length below unity represents a macro particle with partial polarization. Initially, all electrons had spins aligned along the z-axis, which rotated to the y-axis after passing through the Wien filters. The spin angle was calculated using:

$$\theta = \arctan\left(\frac{\langle S_y \rangle}{\langle S_z \rangle}\right) \tag{74}$$

As illustrated in Fig. 6a, the spin direction of the beam rotates from the z-axis to the y-axis as it passes through the two Wien filters, with each filter contributing a 45° rotation. The ESP was determined using Eq. 42. From the gun to the end of the Wien filter, the ESP decreased by 0.0014. Section IV B discusses that longitudinal space charge effects reduce the polarization by 0.0004, while Table IV shows that transverse space charge effects contribute an additional 0.0004 polarization degradation from the gun to the Wien filter exit. Consequently, the total polarization degradation is calculated to be 0.0008. The simulated polarization degradation is observed to be 80% higher than the analytical prediction.

To investigate this discrepancy, simulations were performed with the space charge effects turned off, while all other parameters remained unchanged. In this scenario, the polarization degradation was found to be at the 10^{-5} level. Additionally, the beam emittance was significantly reduced, and the beam size became much smaller, resulting in the beam experiencing a more uniform field. These findings suggest that the inclusion of emittance effects from space charge tracking and the use of a realistic 3D field are responsible for the additional 80% spin degradation observed in the simulation.

Overall, the contribution of space charge effects to spin degradation remains small, as confirmed by the simulations.

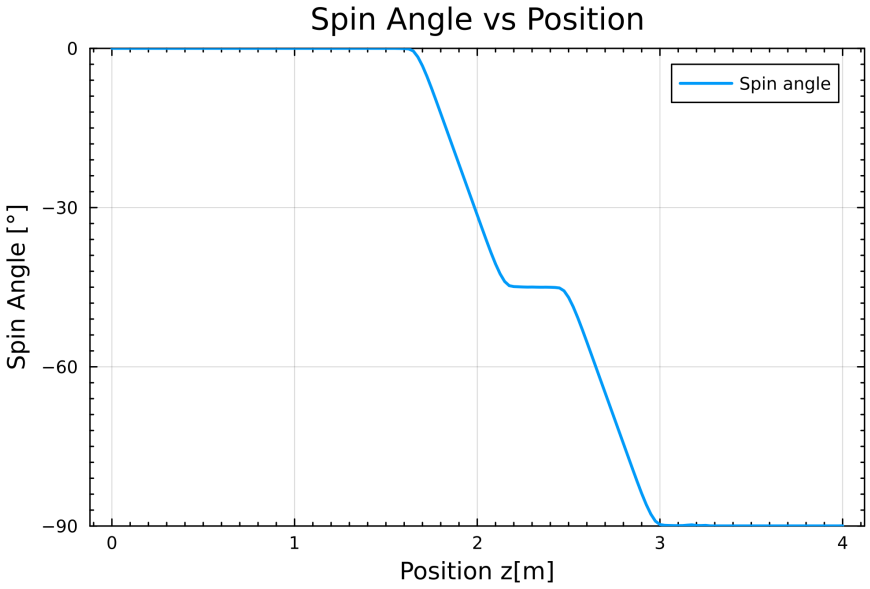

(a) The spin angle from the gun to the exit of Wien filter relevant to beam velocity direction

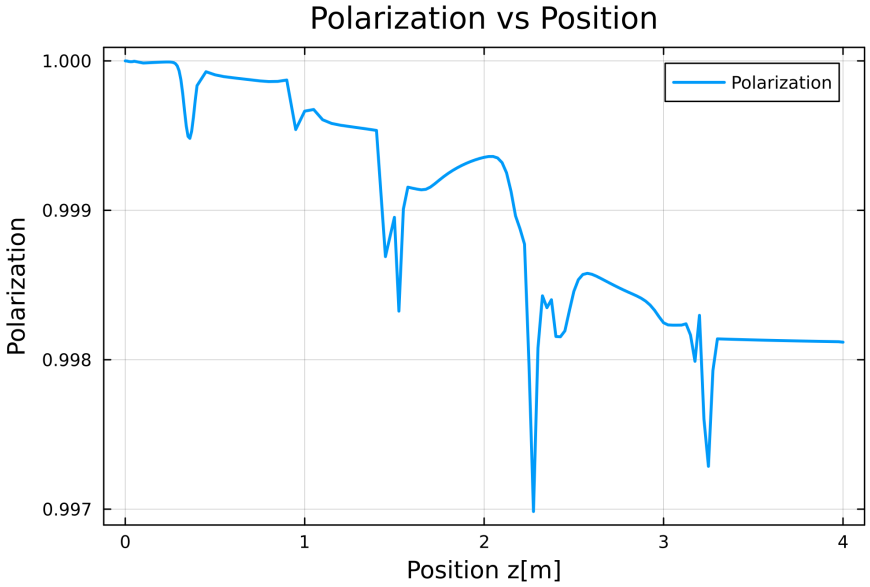

(b) The ESP evolving from the gun to the exit of the Wien filter

FIG. 6: Spin tracking results from the gun to the exit of the Wien filter

VIII. CONCLUSION

The spin rotation of high-charge bunches at low energy is a concern due to the high space charge. In this note, we discuss the impact of space charge on ESP both in the Wien filter section and downstream of it. The longitudinal space charge, which causes energy spread in the bunch, contributes to an ESP degradation of about 4×10^{-4} in the Wien filter range. The transverse space charge causes the following ESP degradations: 4×10^{-4} for the Gun to Wien section, 4×10^{-6} during through the Wien filter, 1×10^{-3} for ballistic compression, and 3×10^{-6} for chicane compression. The overall ESP degradation is between 1×10^{-3} and 2×10^{-3}. The GPT 3.5 spin tracking shows from the gun to the exit of the Wien filter, the ESP degrade 0.0014 which is slightly higher than analytical results due to the included realistic 3D field and beam emittance. These analyses and simulations show that the space charge force's impact on spin polarization degradation is negligible.

IX. ACKNOWLEDGE

We thank Michael Blaskiewicz for reading the manuscript and providing useful suggestions. This work is supported by Brookhaven Science Associates, LLC under Contract No. DE-SC0012704

[1] E. Wang, O. Rahman, J. Biswas, J. Skaritka, P. Inacker, W. Liu, R. Napoli, and M. Paniccia, High-intensity polarized electron gun featuring distributed bragg reflector gaas photocathode, Applied Physics Letters **124**, 254101 (2024), https://pubs.aip.org/aip/apl/article-pdf/doi/10.1063/5.0216694/19998858/254101_1_5.0216694.pdf.

[2] E. Wang, O. Rahman, J. Skaritka, W. Liu, J. Biswas, C. Degen, P. Inacker, R. Lambiase, and M. Paniccia, High voltage dc gun for high intensity polarized electron source, Phys. Rev. Accel. Beams **25**, 033401 (2022).

[3] F. Meot and E. Wang, Spin simulations in erhic wien filter 10.2172/1566292 (2019).

[4] P. A. Adderley, S. Ahmed, T. Allison, R. Bachimanchi, K. Baggett, M. BastaniNejad, B. Bevins, M. Bevins, M. Bickley, R. M. Bodenstein, S. A. Bogacz, M. Bruker, A. Burrill, L. Cardman, J. Creel, Y.-C. Chao, G. Cheng, G. Ciovati, S. Chattopadhyay, J. Clark, W. A. Clemens, G. Croke, E. Daly, G. K. Davis, J. Delayen, S. U. De Silva, M. Diaz, R. Dickson, L. Doolittle, D. Douglas, M. Drury, E. Feldl, J. Fischer, A. Freyberger, V. Ganni, R. L. Geng, C. Ginsburg, J. Gomez, J. Grames, J. Gubeli, J. Guo, F. Hannon, J. Hansknecht, L. Harwood, J. Henry, C. Hernandez-Garcia, T. Hiatt, D. Higinbotham, S. Higgins, A. S. Hofler, J. Hogan, C. Hovater, A. Hutton, C. Jones, K. Jordan, M. Joyce, R. Kazimi, M. Keesee, M. J. Kelley, C. Keppel, A. Kimber, L. King, P. Kjeldsen, P. Kneisel, J. Kowal, G. A. Krafft, G. Lahti, T. Larrieu, R. Lauze, C. Leemann, R. Legg, R. Li, F. Lin, D. Machie, J. Mammosser, K. Macha, K. Mahoney, F. Marhauser, B. Mastracci, J. Matalevich, J. McCarter, M. McCaughan, L. Merminga, R. Michaud, V. Morozov, C. Mounts, J. Musson, R. Nelson, W. Oren, R. B. Overton, G. Palacios-Serrano, H.-K. Park, L. Phillips, S. Philip, F. Pilat, T. Plawski, M. Poelker, P. Powers, T. Powers, J. Preble, T. Reilly, R. Rimmer, C. Reece, H. Robertson, Y. Roblin, C. Rode, T. Satogata, D. J. Seidman, A. Seryi, A. Shabalina, I. Shin, C. Slominski, R. Slominski, M. Spata, D. Spell, J. Spradlin, M. Stirbet, M. L. Stutzman, S. Suhring, K. Surles-Law, R. Suleiman, C. Tennant, H. Tian, D. Turner, M. Tiefenback, O. Trofimova, A.-M. Valente, H. Wang, Y. Wang, K. White, C. Whitlatch, T. Whitlatch, M. Wiseman, M. J. Wissman, G. Wu, S. Yang, B. Yunn, S. Zhang, and Y. Zhang, The continuous electron beam accelerator facility at 12 gev, Phys. Rev. Accel. Beams **27**, 084802 (2024).

[5] G. Palacios Serrano *et al.*, High Voltage Design and Evaluation of Wien Filters for the CEBAF 200 keV Injector Upgrade, JACoW **IPAC2021**, MOPAB324 (2021).

[6] B. Steiner, W. Ackermann, W. Muller, and T. Weiland, Wien filter as a spin rotator at low energy, 2007 IEEE Particle Accelerator Conference (PAC) , 170 (2007).

[7] V. Tioukine and K. Aulenbacher, Operation of the mami accelerator with a wien filter based spin rotation system, Nuclear Instruments and Methods in Physics Research Section A: Accelerators, Spectrometers, Detectors and Associated Equipment **568**, 537 (2006).

[8] E. Wang, J. Skaritka, J. Biswas, and V. Ranjbar, The design progress of a high charge low energy spread polarized pre injector for Electron Ion Collider, JACoW **IPAC2024**, MOPC24 (2024).

[9] V. Bargmann, L. Michel, and V. L. Telegdi, Precession of the polarization of particles moving in a homogeneous electromagnetic field, Phys. Rev. Lett. **2**, 435 (1959).

[10] E. Wang and M. Blaskiewicz, Longitudinal space charge kick in coherent electron cooling 10.2172/1725767 (2020).

[11] G. Stupakov and Z. Huang, Space charge effect in an accelerated beam, Phys. Rev. ST Accel. Beams **11**, 014401 (2008).

[12] M. Ferrario, M. Migliorati, and L. Palumbo, Space Charge Effects, in *CERN Accelerator School: Advanced Accelerator Physics Course* (2014) pp. 331–356, arXiv:1601.05214 [physics.acc-ph].

[13] S. van der Geer, General particle tracer v3.5.

[14] J. Biswas, E. Wang, O. Rahman, J. Skaritka, A. Masters, S. Marsillac, and T.-D. Li, Polarized photocathode r&d at bnl and spin consideration for the eic preinjector, 20th International Workshop on Polarized Sources, Targets, and Polarimetry (PSTP 2024) (2024).